Image-guided Lateral Suboccipital Approach: Part 1—Individualized Landmarks for Surgical Planning

Alireza Gharabaghi, M.D.
Eberhard Karls University Hospital, Tübingen, Germany, and International Neuroscience Institute, Hannover, Germany

Steffen K. Rosahl, M.D., Ph.D.
Helios Hospital, Erfurt, Germany

Günther C. Feigl, M.D.
Eberhard Karls University Hospital, Tübingen, Germany

Thomas Liebig, M.D.
Technical University Hospital, Munich, Germany

Javad M. Mirzayan, M.D.
Medical University Hospital, Hannover, Germany

Stefan Heckl, M.D.
Eberhard Karls University Hospital, Tübingen, Germany

Ramin Shahidi, Ph.D.
Image Guidance Laboratories, Stanford University, Palo Alto, California

Marcos Tatagiba, M.D., Ph.D.
Eberhard Karls University Hospital, Tübingen, Germany

Madjid Samii, M.D., Ph.D.
International Neuroscience Institute, Hannover, Germany

Reprint requests:
Alireza Gharabaghi, M.D., Department of Neurosurgery, University Hospital Tübingen, Charlottenstr. 37/1, 72070 Tübingen, Germany.
Email: alireza.gharabaghi@uni-tuebingen.de

Received, February 25, 2006.
Accepted, January 26, 2007.

OBJECTIVE: Being situated close to the transverse and sigmoid sinus, the asterion has traditionally been viewed as a landmark for surgical approaches to the posterior fossa. Cadaveric studies, however, have shown its variability in relation to underlying anatomic structures. We have used an image-guidance technology to determine the precise anatomic relationship between the asterion and the underlying transverse-sigmoid sinus transition (TST) complex in patients scheduled for posterior fossa surgery. The applicability of three-dimensional (3-D) volumetric image-rendering for presurgical anatomic identification and individualization of a surgical landmark was evaluated.

METHODS: One-millimeter computed tomographic slices were combined with venous computed tomographic angiography in 100 patients, allowing for 3-D volumetric image-rendering of the cranial bone and the dural vasculature at the same time. The spatial relationship between the asterion and the TST was recorded bilaterally by using opacity modulation of the bony surface. The location of both the asterion and the TST could be confirmed during surgery in all of these patients.

RESULTS: It was possible to accurately visualize the asterion and the sinuses in a single volumetrically rendered 3-D image in more than 90% of the patients. The variability in the anatomic position of the asterion as shown in cadaveric studies was confirmed, providing an individualized landmark for the patients. In this series, the asterion was located from 2 mm medial to 7 mm lateral and from 10 mm inferior to 17 mm superior to the TST, respectively.

CONCLUSION: Volumetric image-rendering allows for precise in vivo measurements of anatomic distances in 3-D space. It is also a valuable tool for assessing the validity of traditional surgical landmarks and individualizing them for surgical planning.

KEY WORDS: Asterion, Cranial base, Image-guidance, Sigmoid sinus, Skull base, Surgical anatomy, Three-dimensional surgical planning, Transverse sinus

Neurosurgery 62[ONS Suppl 1]:ONS18–ONS23, 2008 DOI: 10.1227/01.NEU.0000297024.52502.BB

Surface landmarks are widely used for surgical planning and intraoperative orientation. The asterion, the junction of the lambdoid, parietomastoid, and occipitomastoid sutures (4, 27), has been used in posterior fossa surgery to locate the transverse-sigmoid sinus transition (TST) complex (7, 9, 23–26). Because cadaveric studies have shown considerable variability in the relationship of the asterion to the underlying venous structures (8, 29, 33), its validity as a surgical landmark has been questioned (8, 21). Although most experienced surgeons are aware of the limitations of surgical landmarks to predict the precise location of hidden intracranial vasculature, neurosurgeons in training may benefit from new means by which surface landmarks can be reliably translated into surgical approaches. Recent advances in the three-dimensional (3-D) rendering of computed tomographic (CT) images (10, 15) have made it possible to visualize minute bone sutures and venous structures of the posterior fossa at the same time (14, 30). We hypothesize that this technology may provide individualized landmarks that allow surgeons to predict the location of the asterion relating to the TST. Therefore, we have preoperatively studied the in vivo relationship of the asterion

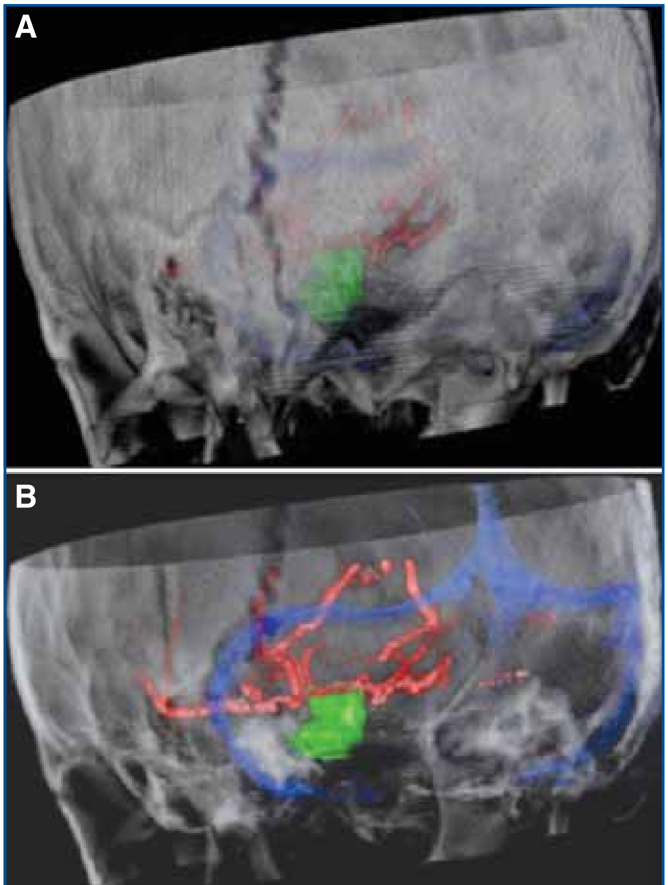

FIGURE 1. **A** *and* **B**, *by gradually decreasing the opacity of the cranium, it is possible to visualize the relationship between the asterion and the transverse–sigmoid transition (*blue*). For better orientation, the circle of Willis (*red*) and a tumor in the cerebellopontine angle (*green*) are highlighted.*

to the underlying TST complex in patients undergoing surgery for cerebellopontine angle lesions and have applied this information to surgical planning.

PATIENTS AND METHODS

One hundred patients (52 male, 48 female; mean age, 48 yr [range, 11–78 yr]) scheduled for posterior fossa surgery (88 vestibular schwannomas, 10 meningiomas, two epidermoids) underwent high-resolution CT scans in combination with venous angiography in a multislice scanner (Somatom Plus 4; Siemens, Erlangen, Germany). Nonionic contrast medium (100 ml of 300 mg/ml solution) was injected with a pump into the cubital vein at a rate of 3.5 ml/s. After a patient-specific delay determined by a bolus test (28–37 s), 100 to 120 consecutive scans were obtained in 1-mm thick slices at 1 mm/s table-forward speed (1024 $\times$ 1024 matrix, 120 kV, and 240 mA). The radiation dose was calculated for each patient by using dedicated software (CT-EXPO V 1.2; Medical University Hannover, Hannover, Germany), resulting in a mean effective radiation dose of 7.7 to 11.3 mSv.

The slice thickness of 1 mm is routinely acquired in all cases of lateral suboccipital craniotomies, which are referred to our institutions

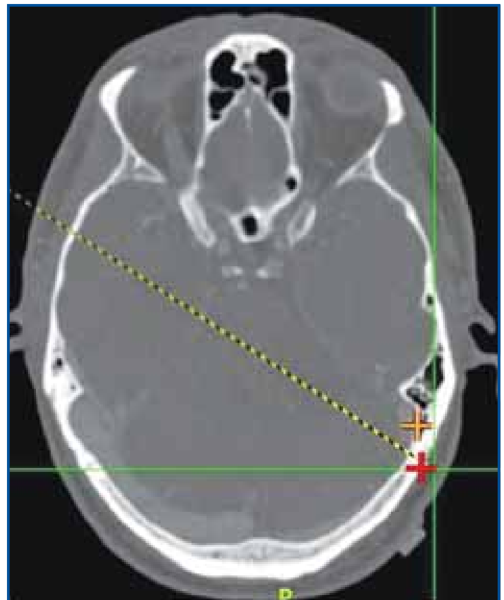

FIGURE 2. *The asterion (*red*) and the "inner knee" of the transverse–sigmoid sinus transition (TST) junction (*orange*) are defined, and their distance is measured in each of the triaxial planes (here the axial plane) using the capabilities of the workstation.*

independent of the purposes of the present study. We preoperatively evaluate the course of emissary veins in the area of the craniotomy as well as the height of the jugular bulb on the side of the intended transmeatal approach. Moreover, we use these high-resolution images to analyze the distance of both the posterior semicircular canal and the crus commune of the labyrinth to the intrameatal tumor extension in relation to the dorsal wall of the internal auditory canal.

For the purpose of this study, the axial source images were transferred to the workstation of a surgical navigation system (Image Guidance Laboratories, Palo Alto, CA). Three-dimensional volumetrically rendered images of the cranium and vasculature were acquired with a minimum density threshold of approximately 60 to 80 HU and a maximum density threshold of 300 to 400 HU.

These volumetric 3-D models allowed for visualization of bony landmarks and venous structures at the same time. The spatial relationship between the asterion and the underlying TST complex was recorded on both sides for each patient, yielding a total of 200 evaluated sides. By varying the perspective of the 3-D model interactively and modulating the transparency of the bony surface, accurate matching of the anatomic structures was achieved.

The morphometric measurement of the anatomic distances was performed in two steps. First, two target points, the asterion and the inner radius ("inner knee") of the TST, were defined within the triaxial images and the same 3-D model by opacity modulation of the cranium bone, allowing for simultaneous visualization of the asterion and the underlying venous structures (*Fig. 1*). To identify the inner knee of the TST, the axial images were viewed in a bottom (caudal) to top (cranial) direction following the course of the sigmoid sinus. As soon as the first slice revealed a connection to the transverse sinus, the image viewer was scrolled one slice back. In this last axial image in which the sigmoid sinus was visible without the transverse sinus, the most posterior and medial part of the sigmoid sinus was defined as the inner knee of the TST (*Fig. 2*, orange crossbar). In the second step, the distances between the target points were measured in each of the triaxial planes by using specific features of the image-guidance software (*Fig. 2*). Thereafter, the imaging findings (the asterion is located above/on top/below the TST) were used for surgical planning and were compared with the intraoperative findings, which served as the "gold standard" regarding the spatial relationship of the asterion to the TST. The accuracy of the image-guidance tool was investigated, calculating the intraoperative target registration error by comparing the in situ position of the navigation probe on a nonregistered fiducial or well-defined bony landmark with the localization of the corresponding site in the reconstructed triaxial images. The mean target registration error amounted to 1.5 mm (± 0.6 mm) over all navigated cases.

RESULTS

Three-dimensional volumetric image-rendering was capable of accurate in vivo visualization of bony and venous structures at the same time in individual patients. The spatial relationship of the asterion and the underlying TST could be determined 91 times on the left side and 92 times on the right side before posterior fossa surgery. In the remaining patients, the sutures were calcified and not visible in the 3-D reconstructions.

The variability of the anatomic position of the asterion shown in cadaveric studies was confirmed in vivo. On the left side, the asterion was located directly over the TST in 59 (65%), above the TST in the supratentorial region in nine (10%), and below the TST complex in 23 (25%) cases, respectively. On the right side, it was located on top of the TST in 68 cases (75%), above the TST in six cases (5%), and below in 18 cases (20%). This information was successfully used for surgical planning of the suboccipital craniotomy.

During surgery, the identified asterion could be related to the intraoperative location of the TST. In all of these patients, the preoperatively image-rendered spatial relationship of the asterion to the TST could be confirmed during surgery regarding the qualitative classification (above/on top/below the TST) (*Fig. 3*; *Table 1*).

In our series, the asterion was located from 2 mm medial to 7.4 mm lateral and from 10 mm inferior to 17 mm superior to the TST, respectively. As a result of this range (−2 to 7.4 and −10 to 17), the calculated mean distances of the asterion to the TST were 2.3 mm lateral and 2.5 mm superior, although the asterion was located inferior and medial to the TST in the vast majority of patients (*Table 1*). The measurements for the right and left sides correlated well and did not differ significantly. The mean distances and standard deviations are shown in *Figure 4*. There was no significant difference for any of the distances with respect to sex, age, or side.

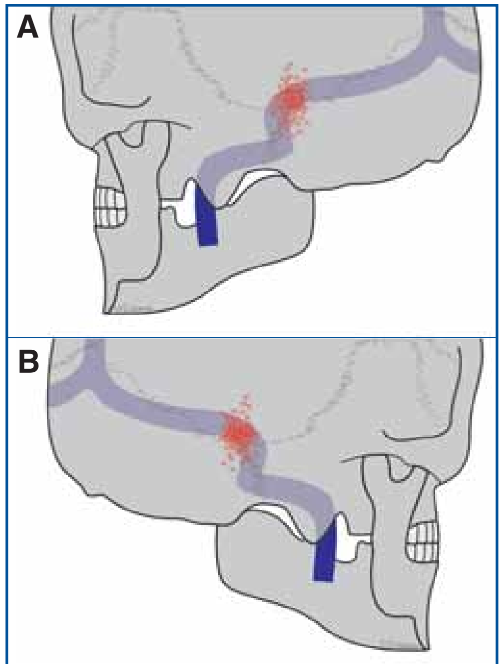

FIGURE 3. *Illustration depicting the lateral view of the TST junction (with mastoid contour for orientation) showing the location of the asterion (91 times for the left [**A**] and 92 times for the right [**B**] side) superimposed on it for each side.*

DISCUSSION

Our results confirm the wide variability of the asterion described in cadaveric studies (*Table 1*) (8, 25, 29, 33). Day and

TABLE 1. Summary of studies on the anatomic position of the asterion in relation to the transverse–sigmoid sinus transition[a,b]

Series (ref. no.)	Study type	Total number of studied sides	Location of the asterion (%)					
			Above TST		On TST		Below TST	
			L	R	L	R	L	R
Ribas et al., 1994 (25)	Cadaver	50	2		78		17	
Day and Tschabitscher, 1998 (8)	Cadaver	200	9	7	66	61	25	32
Sripairojkul and Adultrakoon, 2000 (29)	Cadaver	100	9	2	58	74	33	24
Uz et al., 2001 (33)	Cadaver	50	2		54		44	
Present study, 2006	In vivo	200	10	5	65	75	25	20

[a] TST, transverse–sigmoid sinus transition; L, left; R, right.
[b] In the present study, the asterion could be identified in 183 of 200 studied sides.

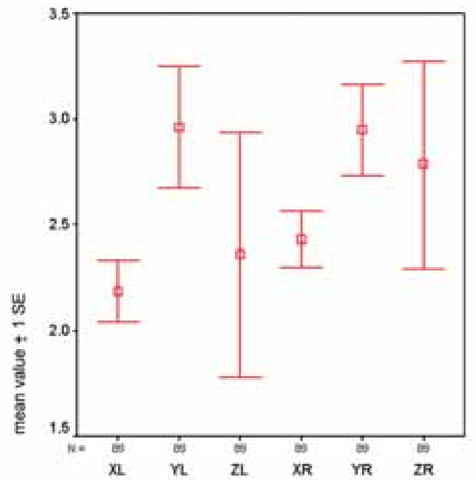

FIGURE 4. *Mean distances (in millimeters) and standard deviations shown between the asterion and the TST in the x-, y-, and z-planes on the left (*Xl, Yl, Zl*) and on the right sides (*Xr, Yr, Zr*), respectively.* SE, *standard error of the mean.*

Tschabitscher (8) found the asterion to be located below the TST complex in 25 and 32% of their cadavers for the left and right sides, respectively. Similar results were described by Sripairojkul and Adultrakoon (29), with the asterion located infratentorially in 33 and 24% of their cases, respectively. Uz et al. (33) found this anatomic position of the landmark in 44% of the cases in their data. With the asterion located below the TST in 25 and 20% of the patients on the left and right sides, respectively, our in vivo data correlate well with these studies.

Based on this background, relying solely on the asterion as a surgical landmark may be hazardous and bears the risk of damaging the dural sinuses when placing a burr hole directly at this point (8, 29). Other landmarks have been advocated for approaches to the posterior fossa (7, 20, 23, 26, 28, 32).

In a cadaver study, Lang and Samii (20) found that if the burr hole was placed 45 mm behind the suprameatal line and 7 mm below the Frankfurt horizontal plane, no sinus opened in 92% of the cases in a series of 37 cases. Rhoton (23) recommended placement of the initial burr hole 2.0 cm below the asterion, two-thirds behind, and one-third in front of the occipitomastoidal suture to avoid the posterior margin of the sigmoid sinus.

Day et al. (7) advocated the superior nuchal line connecting the root of the zygoma with the inion as a landmark for the distal transverse sinus and the transverse–sigmoid junction. From their studies in 100 crania, Day and Tschabitscher (8) recommended placement of the burr hole inferior to this line and just behind the ridge that delimits the body of the mastoid bone.

Malis (21) suggested drilling 2 cm medial to the mastoid tip. Sekhar (28) advised placing the first burr hole inferior and medial to a line drawn from the inion to the base of the mastoid process. Tubbs et al. (32) recommended using the insertion of the semispinalis capitis muscle as a landmark for the proximal transverse sinus. They found that the insertion of the musculus semispinalis capitis corresponded with the transverse sinus in 80 to 93% of cases in a study of 15 cadaveric specimens. Finally, Ribas et al. (26) suggested the most posterior part of the parietomastoid suture and the occipitomastoid suture at the level of the mastoid notch as proper initial burr hole sites.

New anatomic studies may bring to light new surface landmarks with less variability (20, 26, 33). The limitation in these studies is that their conclusions are derived from statistical data in a limited number of cadaveric specimens. For clinical practice, as a result of the wide individual variability of the distances, patient-specific anatomic information is desirable. For morphometric investigations with a larger number of cases, it would be helpful to have an accurate methodology that avoids cadaveric dissection by hand.

With modern technology, CT and magnetic resonance imaging scans yield reliable morphometric data in individual patients (7). Current advances in image-rendering have made it possible to generate precise 3-D models by the reconstruction of image data (2, 16, 19). Three-dimensional CT angiography has been developed and applied for diagnostic and therapeutic purposes (6, 13, 31).

Although image-based stereoscopic virtual reality models are already in use for planning specific surgical procedures and for teaching purposes in neurosurgery (3, 5, 12, 17, 18), most studies that evaluate preoperative neurosurgical planning have focused on 3-D visualization capabilities of the applied software (1, 11, 22, 34, 35). Although several 3-D models simultaneously showing the surface of the cranial bone and venous vasculature of the posterior fossa have been published (14, 30), the gradual, interactive modulation of opacity used to detect minute bone sutures in this study and their relationship to the underlying dural sinuses is a new feature.

By using this technique, the spatial relationship of the asterion and the underlying TST complex was clearly identified in more than 90% of the cases. It was the basis for precise anatomic measurements that can be performed in vivo with the option of generating individualized patient-specific morphometric data in a clinical setting. When validated with these data, the asterion can still be used for surgical planning by determining the patient-specific coordinates of this landmark. Alternatively, the sinuses themselves may be turned into landmarks that are projected onto the surface of the cranium by intraoperative image guidance. This would allow the use of CT angiogram rather than magnetic resonance angiogram, thereby avoiding x-ray exposure. With respect to surgical training, however, it must be kept in mind that the new technology cannot replace hands-on anatomic study.

CONCLUSION

Volumetric 3-D image-rendering appears to be a valuable tool for the validation of surface anatomic landmarks in individual patients and for basic morphometric investigations. More specifically, a simultaneous visualization and interactive modulation of bony surfaces and vascular structures is a suitable method for determining the relationship of the asterion to the underlying TST complex, thereby providing an individualized landmark for surgical planning. Using this imaging technique, the asterion may be revived as a surgical landmark, provided that its individual relationship to the dural sinuses is known to the surgeon from previous imaging. Interactive opacity modulation in volumetrically rendered 3-D images offers new options for anatomic research and morphometric investigations.

REFERENCES

1. Abrahams JM, Saha PK, Hurst RW, LeRoux PD, Udupa JK: Three-dimensional bone-free rendering of the cerebral circulation by use of computed tomographic angiography and fuzzy connectedness. **Neurosurgery** 51:264–269, 2002.
2. Aoki S, Sasaki Y, Machida T, Ohkubo T, Minami M, Sasaki Y: Cerebral aneurysms: Detection and delineation using 3-D-CT angiography. **AJNR Am J Neuroradiol** 13:1115–1120, 1992.
3. Balogh A, Preul MC, Schornak M, Hickman M, Spetzler RF: Intraoperative stereoscopic QuickTime Virtual Reality**. J Neurosurg** 100:591–596, 2004.
4. Bannister LH, Berry MM, Collins P, Dyson M, Dussek JE, Ferguson MWJ (eds): *Gray's Anatomy*. New York, Churchill Livingstone, 1995, ed 38, p 56.
5. Bernardo A, Preul MC, Zabramski JM, Spetzler RF: A three-dimensional interactive virtual dissection model to simulate transpetrous surgical avenues. **Neurosurgery** 52:499–505, 2003.
6. Castillo M, Wilson JD: CT angiography of the common carotid artery bifurcation: Comparison between two techniques and conventional angiography. **Neuroradiology** 36:602–604, 1994.
7. Day JD, Kellogg JX, Tschabitscher M, Fukushima T: Surface and superficial surgical anatomy of the posterolateral cranial base: Significance for surgical planning and approach. **Neurosurgery** 38:1079–1084, 1996.
8. Day JD, Tschabitscher M: Anatomic position of the asterion. **Neurosurgery** 42:198–199, 1998.
9. Hakuba A, Nishimura S, Jang BJ: A combined retroauricular and preauricular transpetrosal–transtentorial approach to clivus meningiomas. **Surg Neurol** 30:108–116, 1988.
10. Harbaugh RE, Schlusselberg DS, Jeffery R, Hayden S, Cromwell LD, Pluta D, English RA: Three-dimensional computed tomographic angiography in the preoperative evaluation of cerebrovascular lesions. **Neurosurgery** 36:320–327, 1995.
11. Hayashi N, Endo S, Shibata T, Ikeda H, Takaku A: Neurosurgical simulation and navigation with three-dimensional computer graphics. **Neurol Res** 21:60–66, 1999.
12. Henn JS, Lemole GM Jr, Ferreira MA, Gonzalez LF, Schornak M, Preul MC, Spetzler RF: Interactive stereoscopic virtual reality: A new tool for neurosurgical education. Technical note. **J Neurosurg** 96:144–149, 2002.
13. Hsiang JN, Liang EY, Lam JM, Zhu XL, Poon WS: The role of computed tomographic angiography in the diagnosis of intracranial aneurysms and emergent aneurysm clipping. **Neurosurgery** 38:481–487, 1996.
14. Kaminogo M, Hayashi H, Ishimaru H, Morikawa M, Kitagawa N, Matsuo Y, Hayashi K, Yoshioka T, Shibata S: Depicting cerebral veins by three-dimensional CT angiography before surgical clipping of aneurysms. **AJNR Am J Neuroradiol** 23:85–91, 2002.
15. Kato Y, Sano H, Katada K, Ogura Y, Hayakawa M, Kanaoka N, Kanno T: Application of three-dimensional CT angiography (3D-CTA) to cerebral aneurysms. **Surg Neurol** 52:113–122, 1999.
16. Kikinis R, Gleason PL, Moriarty TM, Moore MR, Alexander E 3rd, Stieg PE, Matsumae M, Lorensen WE, Cline HE, Black PM, Jolesz FA: Computer-assisted interactive three-dimensional planning for neurosurgical procedures. **Neurosurgery** 38:640–651, 1996.
17. Kockro RA, Serra L, Tsai YT, Chan C, Sitoh YY, Chua GG, Hern N, Lee E, Hoe LY, Nowinski W: Planning of skull base surgery in the virtual workbench: Clinical experiences. **Stud Health Technol Inform** 62:187–188, 1999.
18. Kockro RA, Serra L, Tseng-Tsai Y, Chan C, Yih-Yian S, Gim-Guan C, Lee E, Hoe LY, Hern N, Nowinski WL: Planning and simulation of neurosurgery in a virtual reality environment. **Neurosurgery** 46:118–137, 2000.
19. Koyama T, Okudera H, Kobayashi S: Computer-assisted geometric design of cerebral aneurysms for surgical simulation. **Neurosurgery** 36:541–547, 1995.
20. Lang J Jr, Samii A: Retrosigmoid approach to the posterior cranial fossa: An anatomical study. **Acta Neurochir (Wien)** 111:147–153, 1991.
21. Malis LI: Anatomical position of the asterion. **Neurosurgery** 42:198–199, 1998.
22. Mamata H, Komiya T, Muro I, Matsuyama S: Application and validation of three-dimensional data sets from a phase contrast MR angiography for preoperative computer simulation of brain tumors. **J Magn Reson Imaging** 10:102–106, 1999.
23. Rhoton AL Jr: Surface and superficial surgical anatomy of the posterolateral cranial base: Significance for surgical planning and approach. **Neurosurgery** 38:1083–1084, 1996.
24. Rhoton AL Jr: The cerebral veins. **Neurosurgery** 51 [Suppl 4]:S159–S205, 2002.
25. Ribas GC, Rhoton AL Jr, Cruz OR, Peace D: Temporo-parieto-occipital burr-hole sites study and systematized approaches proposal, in Samii M (ed): *Skull Base Surgery: Anatomy, Diagnosis and Treatment*. Basel, Karger, 1994, pp 723–730.
26. Ribas GC, Rhoton AL Jr, Cruz OR, Peace D: Suboccipital burr holes and craniectomies. **Neurosurg Focus** 19:E1, 2005.
27. Seeger W: *Planning Strategies of Intracranial Microsurgery*. Berlin, Springer-Verlag, 1986.
28. Sekhar LN: Anatomical position of the asterion. **Neurosurgery** 42:198–199, 1998.
29. Sripairojkul B, Adultrakoon A: Anatomical position of the asterion and its underlying structure. **J Med Assoc Thai** 83:1112–1115, 2000.
30. Suzuki Y, Ikeda H, Shimadu M, Ikeda Y, Matsumoto K: Variations of the basal vein: Identification using three-dimensional CT angiography. **AJNR Am J Neuroradiol** 22:670–676, 2001.
31. Tampieri D, Leblanc R, Oleszek J, Pokrupa R, Melancon D: Three-dimensional computed tomographic angiography of cerebral aneurysms. **Neurosurgery** 36:749–755, 1995.
32. Tubbs RS, Salter G, Oakes WJ: Superficial surgical landmarks for the transverse sinus and torcular herophili. **J Neurosurg** 93:279–281, 2000.
33. Uz A, Ugur HC, Tekdemir I: Is the asterion a reliable landmark for the lateral approach to posterior fossa? **J Clin Neurosci** 8:146–147, 2001.
34. Villavicencio AT, Leveque JC, Bulsara KR, Friedman AH, Gray L: Three-dimensional computed tomographic cranial base measurements for improvement of surgical approaches to the petrous carotid artery and apex regions. **Neurosurgery** 49:342–353, 2001.
35. Zhao JC, Chen C, Rosenblatt SS, Meyer JR, Edelman RR, Batjer HH, Ciric IS: Imaging the cerebrovascular tree in the cadaveric head for planning surgical strategy. **Neurosurgery** 51:1222–1228, 2002.

COMMENTS

Gharabaghi et al. have used a new concept that is very clever and will improve surgical flow and safety: they present a novel way of using individual landmarks and apply it to the asterion. The findings confirm previous cadaveric data regarding the variability of the relationship between the sinus and the asterion. The main point is, however, a completely new way of approaching this kind of surgical landmark. The authors determined the relationship between the asterion and the sinus in each individual patient (which was possible in 90% of the patients). The surgeon gets a totally renovated means of knowing how to optimize the craniotomy; in posterior fossa surgery, the optimal placement of the craniotomy is even more sensitive than in other locations. Now it becomes much easier to place the craniotomy in perfect relation to the surgical corridor.

However, I disagree with the authors' interpretation and the interpretation of the success rate as the present technique was applicable in 90% of all patients and should not then be regarded as a 99% successful means of identifying the landmark. In addition, the identification of the pre- and intraoperative findings seem to be slightly repetitive as radiological data and navigation were used in both instances.

The conclusion still remains that this technique is clever and creative; the invention is seemingly simple. Even though the technology and patients have been available, nobody else thought of this technique.

Tiit Mathiesen
Stockholm, Sweden

The authors deal with an issue as old as neurosurgery itself—how does one approach the posterior fossa safely and what landmarks does one use for orientation? The asterion has been defined traditionally as such a landmark, even though, as the authors thoroughly demonstrated, multiple studies have proven a variance in relative location between asterion and underlying risk structures. To record the spatial relationship of these structures individually, the authors evaluated the usefulness of combined three-dimensional volumetric rendering of the skull and venous structures in this study. The authors could demonstrate that the method presented was feasible for locating the asterion in more than 90% of the patients evaluated and reconfirmed a wide variability of its relative anatomic location. The visualization software used by the authors allows for the gradual modulation of opacity of the skull, facilitating the detection of bone sutures. This feature obviously enhanced the localization of the asterion and relates to the high detection rates of this landmark in their series.

The documented anatomic variability, the related risks of pure landmark-orientation, and the detrimental effects of severing the sinus, leading to air embolism, should propel any efforts that reduce surgical morbidity. As a result, this article offers further proof that image guidance is an essential tool to circumnavigate risk to structures while approaching the actual region of interest in the posterior fossa, whether it may be simply in the planning phase or preferentially intraoperatively, by use of a neuronavigation system.

Thomas Gasser
Volker Seifert
Frankfurt, Germany

The authors add to the extensive literature indicating that the asterion is an unreliable surface landmark for the transverse sinus. I use the bump of bone formed by the intersection of the ridge behind the mastoid groove and the superior nuchal line (understanding this term to mean the superior border of the insertion of the cervical musculature) as a rough landmark for the burr hole for this approach. In my mind, angling the perforator so that the hub of the drill is posteroinferior to the bit is at least as important as the precise location of the burr hole. This angling allows the initial penetration of the bit through the bone (and the potential dural laceration) to be most likely over the posterior fossa dura rather than over the sinus.

I am not sure from where the misconception about the value of the asterion as a surface landmark for safe burr hole placement arose. Neither the early descriptions of trephining for septic thrombophlebitis of the lateral sinus (1, 2) nor Dandy's publications on unilateral suboccipital craniotomy (3, 4) mention the asterion explicitly. The illustrations in these influential publications do sometimes show the asterion as located inferior to the sinus (2, 4); perhaps this is the source of the mistaken belief. The same error can be found in modern illustrations as well (5).

Fred G. Barker II
Boston, Massachusetts

1. Arbuthnot LW: The treatment of pyaemia consequent upon disease of the middle ear and unassociated with thrombosis of the lateral sinus. **Br Med J** 1:1480–1481, 1890.
2. Ballance CA: On the removal of pyaemic thrombi from the lateral sinus. **Lancet** 1:1057–1061, 1890.
3. Dandy W: An operation for the cure of tic douloureux: Partial section of the sensory root at the pons. **Arch Surg** 18:687–734, 1929.
4. Dandy W: *Surgery of the Brain.* Hagerstown, WF Prior, 1945.
5. Lang J: *Skull Base and Related Structures: Atlas of Clinical Anatomy*, Stuttgart, Schattauer, 2001, ed 2.